[16] Back-dissociation of the hydrogen-bonded adducts opens the way for the competing nucleophilic substitutions mentioned in reference [13], involving reattack of $N(CH_3)_3$ at the carbon centers of the freed onium ion. Thus, only a fraction of the back-dissociating hydrogen-bonded adducts collapse again to another hydrogen-bonded adduct.

[17] Interaction of $(CH_3)_3N$ with the ring hydrogen atoms of **II** generates an initial distribution of $[IVa^t] \approx [IVs^t]$ which is not far from that corresponding to the thermodynamic equilibrium ($[IVa^t]_{eq} \approx [IVs^t]_{eq}$). Thus, the slight positive temperature dependence of the **4E:4Z** ratios from **2** reflects the effect of temperature on the ring-opening processes and on the limited $IVs^t \leftrightarrow IVa^t$ interconversion. In contrast, interaction of $(CH_3)_3N$ with the ring hydrogen atoms of the **Is/Ia** pair generates the corresponding adducts in an initial distribution of $[IVa^c]$ and $[IVs^c]$ which is far away from the equilibrium distribution ($[IVs^c]_{eq} > [IVa^c]_{eq}$). In this case, the steeper positive temperature dependence of the **4E:4Z** ratios from **1** is much more sensitive to the effect of temperature on the $IVa^c \rightarrow IVs^c$ conversion, which efficiently competes with the ring-opening reactions.

[18] M. J. Frish, G. W. Trucks, H. B. Schlegel, P. M. W. Gill, B. G. Johnson, M. A. Robb, J. R. Cheeseman, T. A. Keith, G. A. Petersson, J. A. Montgomery, K. Raghavachari, M. A. Al-Laham, V. G. Zakrzewski, J. V. Ortiz, J. B. Foresman, J. Cioslowski, B. B. Stefanov, A. Nanayakkara, M. Challacombe, C. Y. Peng, P. Y. Ayala, W. Chen, M. W. Wong, J. L. Andres, E. S. Repogle, R. Gomperts, R. L. Martin, D. J. Fox, J. S. Binkley, D. J. Defrees, J. Baker, J. P. Stewart, M. Head-Gordon, C. Gonzales, J. A. Pople, *Gaussian 94, Revision E. 2*, Gaussian, Inc., Pittsburg, PA, **1995**.

[19] a) A. D. Becke, *J. Chem. Phys.* **1993**, *98*, 1372, 5648; b) C. Lee, W. Yang, R. G. Parr, *Phys. Rev. B* **1988**, *37*, 785.

[20] C. Gonzales, H. B. Schlegel, *J. Phys. Chem.* **1990**, *94*, 5523.

High Oxidation State Organocobalt Complexes: Synthesis and Characterization of Dihydridodisilyl Cobalt(v) Species[**]

Maurice Brookhart,* Brian E. Grant, Christian P. Lenges, Marc H. Prosenc, and Peter S. White

Recently there has been considerable interest in the organometallic chemistry of late transition metals in high oxidation states. Second- and third-row metals in particular were stabilized in high oxidation states by using organic ligand environments. Certain catalytic reactions mediated by these late metals were proposed to occur through high oxidation

[*] Prof. M. Brookhart, Dr. B. E. Grant, Dipl.-Chem. C. P. Lenges, Dr. M. H. Prosenc, Dr. P. S. White
Department of Chemistry, Venable and Kenan Laboratories
University of North Carolina at Chapel Hill
Chapel Hill, NC 27599-3290 (USA)
Fax: (+1) 919-962-2476
E-mail: mbrookhart@unc.edu

state intermediates, as opposed to the traditionally formulated redox pairs.[1–4] Some of the most thoroughly investigated examples in this class are the high oxidation state neutral iridium(v) and rhodium(v) complexes studied initially by Maitlis et al. such as $[(C_5Me_5)IrMe_4]$,[5] $[(C_5Me_5)Ir(H)_2(SiR_3)_2]$, and $[(C_5Me_5)Rh(H)_2(SiR_3)_2]$[6–10] and the Ir^V complex cation $[(C_5Me_5)IrMe_3L]^+$ reported later by Bergman and Aliamo.[11] Higher oxidation states of first-row metals have been discussed as reactive intermediates, but isolated examples are rare.[12] We showed that cationic cobalt(III) alkyl complexes $[(C_5Me_5)\{P(OMe)_3\}CoR]^+$ are olefin hydrosilylation catalysts and must proceed through the Co^V intermediate $[(C_5Me_5)\{P(OMe)_3\}Co(R)(H)(SiR_3)]^+$ or the Co^{III} intermediate $[(C_5Me_5)\{P(OMe)_3\}Co(R)(\eta^2\text{-}H\text{-}SiR_3)]^+$.[13, 14] Here we report the synthesis and X-ray crystallographic characterization of a bis-hydrido bis-silyl cobalt(v) complex.

For cobalt-mediated bond-activation reactions we have used olefin complexes of the type $[(C_5Me_5)Co(olefin)_2]$ (**1**) as catalysts,[13, 15–17] which provides a source of $[(C_5Me_5)Co]$ through olefin dissociation.[18] Heating a solution of **1a** in C_6D_6 (olefin $= C_2H_4$) with 5 equiv of Ph_2SiH_2 (15 min, 70°C) led to a rapid disappearance of starting material and, along with the appearance of ethylene and $Ph_2(Et)SiH$, the formation of two products **2a** and **3** in approximately 1:1 molar ratio, as determined by ^1H NMR spectroscopy [Eq. (1)].[19] Equivalent hydrido ligands and silyl methylene protons support a *trans* configuration of **2a**, while a single set of ^{13}C phenyl signals indicates a *trans* configuration for **3**.

$$(1)$$
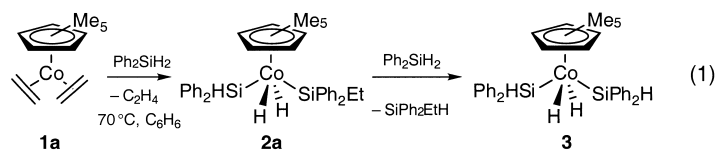
Heating **1a** with an excess of Ph_2SiH_2 (5–10 equiv) in toluene at 85°C for 60 min and removal of volatiles resulted in quantitative formation of **3**. Extraction with pentane and crystallization at $-25°C$ produces white crystals that are stable to air in the solid state and can be stored indefinitely at 20°C in an argon atmosphere. In the temperature range of -80 to 70°C no reactivity or dynamic behavior of **3** was observed by NMR spectroscopy. No exchange or magnetization transfer between the Co–H and the Si–H groups was observed on the NMR timescale, and silicon satellites for the Co–H signals were absent. On the basis of this spectroscopic evidence, the new cobalt silyl hydrido complexes are formulated as rare examples of organocobalt(v) species which contribute to a now complete series of silyl hydride complexes of the type $[(C_5Me_5)M(SiR_3)_2(H)_2]$ (M = Co, Rh, Ir).[6–10]

The activation of the Si–H bond is facile in this process, as is suggested by the reactivity of the more labile cobalt(I) precursor $[(C_5Me_5)Co(C_2H_3SiMe_3)_2]$ (**1b**). The reaction of **1b** with Ph_2SiH_2 (15 equiv) in C_6D_6 at 30°C for 10 h gave a reaction mixture consisting of $[(C_5Me_5)Co(SiPh_2C_2H_4SiMe_3)(SiPh_2H)(H)_2]$ (**2b**) (70%) and a minor amount of **3**. Heating this reaction mixture at 80°C for 2 h resulted in quantitative formation of **3**. The reaction of Ph_2SiH_2 with

$C_2H_3SiMe_3$ in the presence of a catalytic amount of **1b** (5 mol%, 50 °C, 24 h) resulted in only 15% conversion to the hydrosilylation product $Ph_2Si(H)CH_2CH_2SiMe_3$. During this process, **1b** is converted to **3**. This indicates that these new cobalt(v) silyl hydrides are not active at 50 °C in the catalytic hydrosilylation of olefins.[20]

Scheme 1 outlines two possible routes for the formation of **3** from **1a**, **b**. Since intermediates **2a**,**b** are precursors to **3**, the mechanism must incorporate hydrosilylation of one of the olefin ligands of **1a**,**b**. Formation of **5a**,**b** by oxidative addition of silane to **4a**,**b** is certainly the first step. Silyl (path a; Scheme 1) or hydride (path b) migration may occur to produce **6a**,**b** or **7a**,**b**, respectively, which can both be converted to **9a**,**b**. Path b for **5b** is consistent with the previously observed regiochemistry of insertion of vinyl-trimethylsilane into a cobalt–hydrogen bond,[21, 22a] which could be followed by α-elimination and subsequent alkyl–silylene coupling to form **9a**,**b**.[22b] Alternatively, it is reasonable to suggest that the bulky SiPh$_2$H group might migrate to C_β (path a; Scheme 1). Conversion of **7a**,**b** to **9a**,**b** may occur via formation of the metallacycle **8a**,**b**. Oxidative addition of

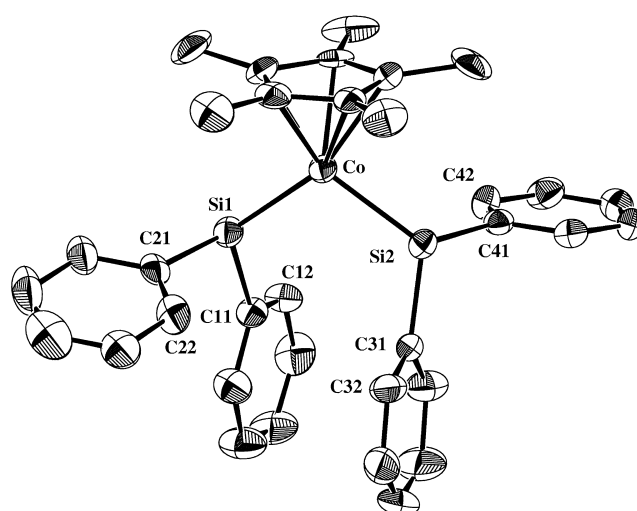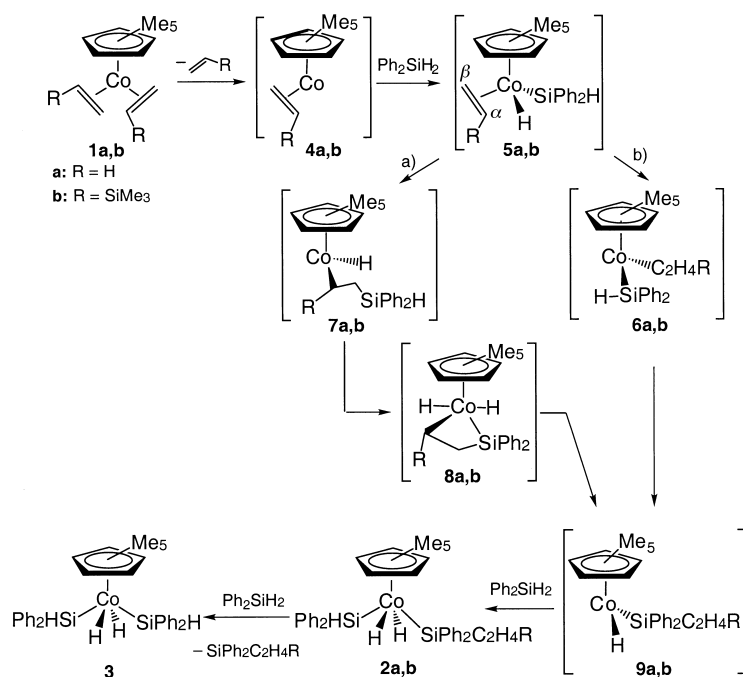
Figure 1. ORTEP diagram of complex **3** (50% probability ellipsoids). Selected bond lengths [Å] and angles [°]: Co–Si1 2.2492(21), Co–Si2 2.2536(19), Si1–C11 1.894(6), Si1–C21 1.922(7), Si2–C31 1.885(7), Si2–C41 1.895(6); Si1-Co-Si2 107.21(8), Co-Si1-C11 117.58(21), Co-Si1-C21 116.58(21), Co-Si2-C31 119.76(21), Co-Si2-C41 117.04(20).

The Co–Si distances[24] are slightly shorter than those of related Co^{III} silyl complexes (2.28–2.30 Å) as expected for the smaller ionic radius of cobalt in the higher oxidation state.[25, 26] The Si1-Co-Si2 angle in **3** of 107.2° is slightly smaller than the corresponding angle of the rhodium complex, and this could be attributed to the larger nonbonding repulsions in the ligands around the smaller Co center. Especially interesting in **3** is the arrangement of the SiPh$_2$H group around the cobalt center. To reduce steric crowding, one of the phenyl groups on each Si atom is oriented parallel to the C$_5$Me$_5$ ligand. The other two phenyl groups are roughly perpendicular (105°) to the C$_5$Me$_5$ ring and parallel to each other with a distance of 3.7 Å between the best planes of the six carbon atoms of each ring. The C-Si-Co angles of 117–120° are significantly larger than 109.5°; we suppose that this also contributes to reduction of nonbonding repulsions around the Co center. Similar large C-Si-Co angles (114–120°) were also found in the calculated structure (see below) in which intermolecular interactions were not taken into account.

Scheme 1. Proposed mechanism for formation of **3** from **1a**,**b**.

Ph_2SiH_2 to **9a**,**b** results in **2a**,**b**.[23] Reductive elimination of $Ph_2Si(C_2H_4R)(H)$ from **2a**,**b** followed by oxidative addition of Ph_2SiH_2 produces **3**.

To support the spectroscopic and chemical evidence for these cobalt(v) complexes, single crystals of **3** were subjected to X-ray structural analysis. The unit cell contains four independent molecules, one of which is shown in Figure 1. The X-ray structure verifies the proposed structure for **3**. The hydrido ligands attached to the cobalt center and the H atoms bound to silicon atoms could not be located in the difference Fourier map. Key structural parameters of **3** are listed in Table 1 and compared to those of related Rh and Ir complexes.

Table 1. Comparison of selected interatomic distances [Å] and bond angles [°] in $[(C_5Me_5)M(H)_2(SiR_3)_2]$ (M = Rh, Ir and SiR$_3$ = SiEt$_3$; M = Co, SiR$_3$ = SiPh$_2$H).

	Ir	Rh	Co[a]	Co[b]
M–Si	2.390(1)	2.379(2)	2.256–2.261	2.29
			2.243–2.247	2.28
M–H	1.581(1)	1.594(1)		1.49
Si–C	1.901(2)	1.900(1)	1.880–1.922	1.90
H1-M-H2	99.50(2)	94.84(2)		100
Si1-M-Si2	109.49(6)	107.90(8)	107.2	109
H1⋯Si1	2.272(2)	2.212(2)		2.24
H2⋯Si1	2.384(2)	2.336(2)		2.25
H1⋯H2	2.433(4)	2.328(4)		2.28

[a] Averaged for the four molecules in the unit cell. [b] Data are based on DFT calculations (see text).

To further investigate structural details of complex **3**, density functional theory (DFT) calculations were conducted[27–30], as were successfully employed for related organometallic complexes.[31–34] Some geometrical parameters obtained after geometry optimization are listed in Table 1. The main structural features of the calculated geometry of **3** and the X-ray structure of **3** are in good agreement. The Co–Si bond lengths in the calculated structure (Co–Si 2.29 Å) are slightly longer than those observed experimentally (Co–Si 2.26 Å). The pseudo-square-pyramidal structure of the ML$_5$ complex is clearly evident from the calculation. The calculated H–H distance for complex **3** of 2.28 Å and the H–Si distances of 2.24 and 2.25 Å indicate the complete oxidative addition of the two Ph$_2$SiH$_2$ molecules to the cobalt center.[35]

We compared the Co^V species **3** with other high oxidation state silyl hydrido complexes. Interestingly, the rare iron(IV) complex **10** also has a *trans* configuration around the Fe center.[36] Complex **11**, an Ru analogue of **3**, was recently reported[37] and also structurally characterized.
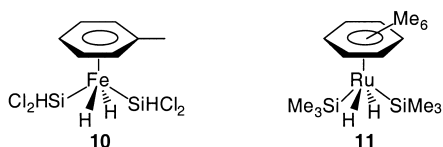
In summary, we have prepared and structurally characterized rare examples of organometallic Co complexes in the formal oxidation state +5. Our DFT calculations fully support the assigned structure and oxidation state of these cobalt complexes. These species are remarkably stable towards reductive elimination, and this is consistent with the well-established ability of silyl and hydrido ligands to stabilize metals in high oxidation states.

Experimental Section

All operations were carried out under an Ar atmosphere. All solvents were degassed and purified by standard methods.

3: Ten equivalents of diphenylsilane were added to a solution of **1a** (0.15 g, 0.6 mmol) in toluene (5 mL). The mixture was stirred for 1 h at 80 °C. After cooling to 20 °C and removal of all volatile materials, the resulting solids were dissolved in pentane and filtered. The clear, pale yellow solution was cooled to −78 °C for 24 h; white crystalline material was obtained (72 % yield). Crystals for the X-ray structure analysis were obtained from pentane at −25 °C.

Spectroscopic data for **3**: ^{1}H NMR (300 MHz, [D$_6$]benzene, 20 °C) $\delta = 1.53$ (s, 15 H, C$_5$Me$_5$), 5.92 (s, 2 H, Si–H), 7.15 (m, 12 H, Ph), 7.71 (m, 8 H, Ph) −15.51 (s, 2 H, Co–H); ^{13}C{^{1}H} NMR: $\delta = 95.46$ (C$_5$Me$_5$), 9.65 (C$_5$Me$_5$), 140.90, 136.40, 135.88, 134.99 (Ar); elemental analysis: calcd: H 6.99, C 72.57; found: H 7.11, C 72.32.

Structural data for **3**: crystals from pentane; C$_{34}$H$_{39}$Si$_2$Co, $M_r = 562.76$; monoclinic, space group C_c; $Z = 16$; $a = 60.673(3)$, $b = 10.0978(5)$, $c = 20.8573(10)$ Å, $\beta = 109.264(1)°$, $V = 12063.1(10)$ Å^3; $\rho_{calcd} = 1.235$ g cm^{-1}; $T = −110 °C$; $2\theta_{max} = 50°$; Mo$_{K\alpha}$ radiation ($\lambda = 0.71073$ Å), 50673 reflections were measured; 21315 unique reflections were obtained, and 14248 of these with $I > 3.0\sigma(I)$ were used in the refinement; data were collected on a Siemens SMART diffractometer by the Ω scan method. For significant reflections, the merging R value was 0.052; residuals: $R_F = 0.046$, $R_w = 0.054$ (significant reflections); GOF 1.42. Crystallographic data (excluding structure factors) for the structures reported in this paper have been deposited with the Cambridge Crystallographic Data Centre as supple-

mentary publication no. CCDC-136182. Copies of the data can be obtained free of charge on application to CCDC, 12 Union Road, Cambridge CB21EZ, UK (fax: (+44)1223-336-033; e-mail: deposit@ccdc.cam.ac.uk).

[1] Pd-catalyzed Heck reactions were recently explained by invoking Pd^{IV} intermediates; see for example: M. Ohff, A. Ohff, M. E. van der Boom, D. Milstein, *J. Am. Chem. Soc.* **1997**, *119*, 11687.

[2] Shilov-type alkane oxidation involves Pt(IV) intermediates: J. E. Bercaw, J. A. Labinger, S. Stahl, *Angew. Chem.* **1998**, *110*, 2298; *Angew. Chem. Int. Ed.* **1998**, *37*, 2180.

[3] Hydrosilylation of olefins was explained by invoking Rh^V intermediates: R. N. Perutz, S. B. Duckett, *Organometallics* **1992**, *11*, 90.

[4] The dehydrogenative coupling of arenes and silanes is catalyzed by the Rh^V complex [C$_5$Me$_5$Rh(H)$_2$(SiEt$_3$)$_2$]: K. Ezbiansky, P. I. Djurovich, M. LaForest, D. J. Sinning, R. Zayes, D. H. Berry, *Organometallics* **1998**, *11*, 1455.

[5] P. M. Maitlis, N. Dudeney, O. N. Kirchner, J. C. Green, *J. Chem. Soc. Dalton Trans.* **1984**, 1877.

[6] T. F. Koetzle, J. S. Ricci, P. M. Maitlis, M.-J. Fernandez, *J. Organomet. Chem.* **1986**, *299*, 383.

[7] P. M. Maitlis, C. M. Spencer, B. E. Mann, J. Ruiz, P. O. Bentz, *J. Chem. Soc. Chem. Commun.* **1985**, 1985.

[8] P. M. Maitlis, M.-J. Fernandez, *Organometallics* **1983**, *2*, 164.

[9] P. M. Maitlis, M.-J. Fernandez, *J. Chem. Soc. Chem. Commun.* **1982**, 1982.

[10] P. M. Maitlis, B. F. Taylor, C. M. Spencer, B. E. Mann, J. Ruiz, *J. Chem. Soc. Dalton Trans.* **1987**, 1963.

[11] P. J. Aliamo, R. G. Bergman, *Organometallics* **1999**, *18*, 2707.

[12] Rare Co^{IV} and Co^V tetrakis(1-norbornyl) complexes have been isolated: a) B. K. Bower, H. G. Tennent, *J. Am. Chem. Soc.* **1972**, *94*, 2512; b) E. K. Byrne, D. S. Richeson, K. H. Theopold, *J. Chem. Soc. Chem. Commun.* **1986**, 1491; c) E. K. Byrne, K. H. Theopold, *J. Am. Chem. Soc.* **1987**, *109*, 1282.

[13] M. Brookhart, B. E. Grant, *J. Am. Chem. Soc.* **1993**, *115*, 2151.

[14] Bergman et al. discussed a similar mechanistic controversy in C–H activation reactions mediated by cationic Ir complexes: P. Burger, R. G. Bergman, *J. Am. Chem. Soc.* **1993**, *115*, 10462; see also ref. [11].

[15] C. P. Lenges, P. S. White, M. Brookhart, *J. Am. Chem. Soc.* **1998**, *120*, 6965.

[16] C. P. Lenges, P. S. White, M. Brookhart, *Angew. Chem.* **1999**, *111*, 535; *Angew. Chem. Int. Ed.* **1999**, *38*, 552.

[17] C. P. Lenges, B. E. Grant, M. Brookhart, *J. Organomet. Chem.* **1997**, *528*, 199.

[18] J. L. Spencer, R. G. Beevor, S. A. Frith, *J. Organomet. Chem.* **1981**, *221*, C25.

[19] ^{1}H NMR (300 MHz, [D$_6$]benzene, 20 °C) of **2a**: $\delta = 5.92$ (s, 2 H, Si–H), 1.41 (s, 15 H, C$_5$Me$_5$), −16.0 (s, 2 H, Co–H), and triplet and quartet signals diagnostic of a (silyl)ethyl group. For **3**, see Experimental Section.

[20] Interestingly **1b** is an active catalyst for the hydrosilylation of aromatic ketones with HSiEt$_3$; however, hydrosilylation with Ph$_2$SiH$_2$ is not observed, and complex **3** is generated instead. Complex **3** is not significantly active in catalytic hydrosilylation of aromatic ketones.

[21] The expected Co^{III} olefin silyl hydrido complex was not observed, and this is in clear contrast to the analogous rhodium(III) complex [(C$_5$Me$_5$)Rh(C$_2$H$_4$)(H)(SiEt$_3$)] prepared by Maitlis et al.[8, 22, 23]. With HSi(OEt)$_3$ as substrate; however, this type of intermediate was observed in a reaction with **1b**: C. P. Lenges, M. Brookhart, unpublished results.

[22] a) Catalytic H/D exchange reactions of **1b** in [D$_6$]benzene result in selective deuteration of the α-position of vinyltrimethylsilane; see ref. [16]; b) the formation of silylenes by α-elimination from silyl hydrides has been discussed, and examples of this reactive species have recently been isolated: G. P. Mitchell, T. D. Tilley, *Angew. Chem.* **1998**, *110*, 2602; *Angew. Chem. Int. Ed.* **1998**, *37*, 2524.

[23] The formation of the Rh silyl hydrido analogues follows a similar mechanism[5–10]. Si–H bond activation occurs after dissociation of DMSO from [(C$_5$Me$_5$)RhMe$_2$(dmso)] to generate a rhodium(V) intermediate: M. Gomez, J. M. Kisenyi, G. J. Sunley, P. M. Maitlis, *J. Organomet. Chem.* **1985**, *296*, 197.

[24] The geometries of the four independent molecules of **3** in the unit cell show very similar values for the Co–Si distances. However, small deviations between 2.25 Å (Co–Si1) and 2.26 Å (Co–Si2) are observed within each molecule in the unit cell.

[25] The steric effect of the more bulky $SiEt_3$ group in the Rh complex elongates the Rh–Si bond distance increasing the expected difference between Rh–Si and Co–Si (see Table 1).

[26] J. Y. Corey, J. Braddock-Wilking, *Chem. Rev.* **1999**, *99*, 175.

[27] For calculations of energies and gradients we used the hybrid nonlocal density functional according to Becke and Lee, Yang, and Parr (B3LYP). For all calculations the program Gaussian94 was used with the fine integration grid option. For geometry optimization a gradient convergence criterion of $0.1 E - 6$ was used. For C, H, and Si we used the 6-31G* split-valence basis set supplied by the program. For Co we used an effective core potential basis set according to Hay and Wadt with double zeta quality in the valence region.

[28] C. Lee, W. Yang, R. G. Parr, *Phys. Rev. Sect. B* **1988**, *37*, 785.

[29] P. J. Hay, W. R. Wadt, *J. Chem. Phys.* **1985**, *82*, 299.

[30] *Gaussian 94*, Revision E.2, Gaussian, Inc., Carnegie Office Park, Building 6, Pittsburgh, PA 15106, USA, **1995**.

[31] M. R. Bloomberg, P. E. M. Siegbahn, M. Svensson, *J. Chem. Phys.* **1996**, *104*, 9546.

[32] P. E. M. Siegbahn, *J. Am. Chem. Soc.* **1996**, *118*, 1487.

[33] R. Poli, K. M. Smith, *Eur. J. Inorg. Chem.* **1999**, 877.

[34] M.-D. Su, S.-Y. Chu, *Chem. Eur. J.* **1999**, *5*, 198.

[35] Orbital population analysis revealed that the main bonding contribution between the metal atom and the hydrido and silyl ligands arises from their σ bonds. A very small π backbonding from a metal d_{xz} orbital into a Si p_x orbital (about 2 % of the σ bond) also contributes to the Co–Si bond. Some contribution to the stability of the complex appears to arise from the overlap population of Si and the hydrido ligands of 0.1 electrons.

[36] K. J. Klabunde, Z. Yao, A. C. Hupton, *Inorg. Chim. Acta* **1997**, *259*, 119.

[37] P. I. Djurovich, P. J. Carroll, D. H. Berry, *Organometallics* **1994**, *13*, 2551.

Traceless, Solid-Phase Synthesis of Biarylmethane Structures through Pd-Catalyzed Release of Supported Benzylsulfonium Salts**

Cécile Vanier, Franz Lorgé, Alain Wagner,* and Charles Mioskowski*

Solid-phase synthesis (SPS) has attracted much attention from the scientific community during the past decade, particularly by pharmaceutical companies in their race to speed up drug discovery. Solid-phase chemistry evolved from peptide chemistry and gradually became a field on its own in chemistry.[1] Multi-step processes were automated in a peptide-like fashion, and gave birth to the so-called high-throughput synthesis (HTS).

[*] A. Wagner, C. Mioskowski, C. Vanier, F. Lorgé
Laboratoire de Synthèse Bio-organique
Université Louis Pasteur de Strasbourg
UMR 7514 associée au CNRS, Faculté de Pharmacie
74, route du Rhin - B. P. 24, 67401 Illkirch cedex (France)
Fax: (+ 33) 3-88-67-88-91
E-mail: Wagner@bioorga.u-strasbg.fr,
    Mioskowski@bioorga.u-strasbg.fr

Under this impulse, new tools for SPS were rapidly developed, for example, new generations of robots and synthesizers, resins, linkers, reactions, and building blocks. However, most of the chemistry performed derives from solution and peptide synthetic studies and do not make full benefit of the use of the solid-support technique. In particular, the most frequently used linkers were designed for peptide-like synthesis. Substrates are therefore linked to the solid support through either an ester, amide, or ether bond. Thus, the cleaved products contain an acid, amide, or hydroxyl residue, respectively, at the former linkage site (Scheme 1, path A).[2]
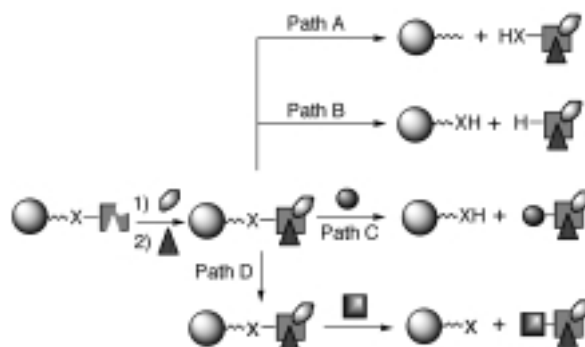
Scheme 1. Anchoring–cleavage strategies used in SPS.

To avoid a residual functionality on the cleaved product, traceless cleavage strategies were developed (Scheme 1 path B).[3] These strategies result in the formation of a carbon–hygrogen or heteroatom–hydrogen bond and often rely on cyclization/cleavage or *ipso*-aromatic-substitution reactions.[4]

Recently developed synthetic procedures for SPS have allowed the introduction of diversity concomitantly with the release of the target compound (Scheme 1, path C).[5] These advantageous double transformations are generally achieved through nucleophilic cleavage. The resin is thus used both as a protecting group during all preliminary SPS steps, and as a leaving group during the cleavage. These two properties, stability during SPS and reactivity towards cleavage, are somewhat antinomic. The linkages so far reported for such functionalizing cleavage suffer from an enhanced reactivity that forbids the use of many reaction conditions during the SPS sequence.

To overcome this drawback a tether that is stable during SPS steps but becomes reactive after selective activation is used (Scheme 1, path D). An example of such a strategy is the safety-catch linker of Kenner et al.,[6] which is unreactive towards nucleophiles as such, but becomes electrophilic upon activation with diazomethane. Other linkers such as the REM or hydrazide linkers were recently developed based on the same principle.[7] Although they allow efficient cleavage, they are highly specific and can not be used generally.

To the best of our knowledge, no strategy so far reported for the safety-catch linkers enables concomitant formation of a carbon–carbon bond and functionalization within the cleavage step. During the course of our study on the SPS of